Environmental and Experimental Botany, Volume 185, May 2021, Article number 104404
DOI:10.1016/j.envexpbot.2021.104404

NCED expression is related to increased ABA biosynthesis and stomatal closure under aluminum stress

Marina Alves Gavassi[1], Giselle Schwab Silva[1], Carolina de Marchi Santiago da Silva[2], Andrew J. Thompson[3], Kyle Macleod[3], Paulo Marcelo Rayner Oliveira[4], Mariana Feitosa Cavalheiro[5], Douglas Silva Domingues[6], Gustavo Habermann[6*]

[1]Programa de Pós-Graduação em Biologia Vegetal, Departamento de Biodiversidade, Instituto de Biociências, Universidade Estadual Paulista, UNESP, Av. 24-A, 1515; 13506-900, Rio Claro, SP, Brazil; [2]Departamento de Ciências Biológicas, Escola Superior de Agricultura "Luiz de Queiróz" Universidade de São Paulo, ESALQ-USP, Av. Pádua Dias, 11, 13418-900, Piracicaba, SP, Brazil; [3]Cranfield Soil and Agrifood Institute, Cranfield University, College Rd, MK43 0AL, Cranfield, United Kingdom; [4]Departamento de Botânica, Instituto de Biocências, Universidade de São Paulo, USP, Rua do Matão, 14, 05508-090, São Paulo - SP, Brazil; [5]Programa de Pós-Graduação em Genética e Biologia Molecular, Centro de Biologia Molecular e Engenharia Genética, Instituto de Biologia, Universidade Estadual de Campinas, Avenida Cândido Rondon, Cidade Universitária, 13083875, Campinas, SP, Brazil [6]Departamento de Biodiversidade, Instituto de Biociências, Universidade Estadual Paulista, UNESP, Av. 24-A, 1515; 13506-900, Rio Claro, SP, Brazil.

** Author for correspondence: Gustavo Habermann, Tel: +0055 (19) 3526-4210, gustavo.habermann@unesp.br*

ABSTRACT

Aluminum (Al)-induced decrease in leaf hydration has been associated with low gas exchange, especially stomatal conductance (g_s). However, the mechanisms explaining these responses are unclear. *Citrus limonia* was exposed to 0 and 1480 μM Al in nutrient solution for 90 days to test whether the low g_s and leaf hydration in plants exposed to Al is associated with increased 9-*cis*-epoxycarotenoid dioxygenase (NCED) gene expression and abscisic acid (ABA) biosynthesis. Relative leaf water content (RWC), water potential (Ψw) and gas exchange in the leaves, as well as leaf and root *ClNCED3*, *ClNCED1* and *ClNCED5* expression and accumulation of ABA and its metabolites (phaseic acid, dihydrophaseic acid, (+)-7′-hydroxy-ABA and ABA-β-D-glucosyl ester) were measured. Al up-regulated *ClNCED3* and induced ABA accumulation in the roots before impairments in leaf water status (low Ψw, RWC and g_s) could be observed. Leaf ABA concentration increased from 7 to 90 days and this could be partially explained by the up-regulation of *ClNCED3*, *ClNCED1* and *ClNCED5* in this organ. Stomatal closure occurred concomitantly with the increase of ABA concentration, and this result provides further evidence of the role of ABA modulation of plant hydration under Al stress.

Keywords: ABA, aluminum, *Citrus*, plant signalling, water relations, NCED genes

1. Introduction

Several studies have shown low stomatal conductance (g_s) in plants under aluminum (Al) toxicity. In comparison to plants not exposed to Al, g_s values may reduce by 80% in *Solanum lycopersicum* (Simon et al., 1994) and *Secale cereale* (Silva et al., 2012), 44% in *Zea mays* (Anjum et al., 2016), 38% in *Hordeum vulgare* (Ali et al., 2011), 30% in *Citrus reshni* ('Cleopatra' tangerine) (Chen et al., 2005b), 40% in *C. grandis* ('Sour Pummelo') (Jiang et al., 2008) and 50% in *C. limonia* ('Rangpur' lime) (Silva et al., 2018).

As g_s is controlled tightly by plant water status (Dodd et al., 2003; Huber et al., 2019), one explanation for the low g_s in plants exposed to Al could be the inhibition of root growth (Kopittke et al., 2008; Singh et al., 2017; Silva et al., 2019). Al-induced reduction in g_s is considered an indirect (long distance) effect of Al because it is nearly all retained in negatively charged pectin nets of root cells (Kopittke et al., 2015). Thus, Al toxicity results in lower root surface area (Panda et al., 2009; Szatanik-Kloc, 2016), reduction in water uptake, water deficiency in the shoot (Tamás et al., 2006; Yang et al., 2013) and low g_s (Vitorello et al., 2005). However, most studies in which Al induced low g_s (Simon et al., 1994; Jiang et al., 2008; Ali et al., 2011; Silva et al., 2012; Banhos et al., 2016; Silva et al., 2018; Cavalheiro et al., 2020) were conducted with plants growing directly on nutrient solution, where water is constantly available. In addition, fibrous xylem vessels (Banhos et al., 2016), more lignin deposition (Silva et al., 2019) and structural damage (Batista et al., 2013) to the root vascular cylinder have been observed in plants under Al toxicity. Aluminum also decreases root hydraulic conductivity in maize plants maintained in nutrient solution (Gunsé et al., 1997), although this study did not measure g_s and neither associated both variables. Furthermore, low leaf water potential (Ψw) and decreased relative leaf water content (RWC) can be observed in plants exposed to Al, even when the plants are grown directly on nutrient solution (Banhos et al., 2016; Silva et al., 2018; Cavalheiro et al., 2020).

Besides low root growth and compromised plant hydraulics, root-to-shoot chemical signalling could also explain low g_s in plants exposed to Al in nutrient solution. For example, abscisic acid (ABA) signalling controls g_s when roots are exposed to Al, but only few studies have examined the role of ABA in plants exposed to Al, and these studies have focused on the role of ABA in root Al resistance, without measuring g_s (Shen et al., 2004; Hou et al., 2010; Reyna-Llorens et al., 2015; Kopittke, 2016). Recent evidence showed that decrease in root hydraulic conductance and increase in ABA could explain Al-induced stomatal closure in tomato plants (Gavassi et al., 2020). ABA strongly controls stomatal movement (Zhang and Davies, 1989; Merilo et al., 2015), and stomatal closure is one of the most studied roles of

ABA in response to drought, high temperature and salt stress (Xiong and Zhu, 2003; Mehrotra et al., 2014). In plants under drought, ABA rapidly accumulates causing low g_s to reduce transpiration (Zhang et al., 2008; Estrada-Melo et al., 2015). Cellular ABA concentration continuously fluctuates, enabling plants to grow while coping with stressful conditions (Ma et al., 2018). ABA concentration is regulated by its biosynthesis (Ng et al., 2014), which originates from the cleavage of xanthophyll precursors, and also its degradation (Xu et al., 2013). The main oxidative route of ABA catabolism is the 8′ hydroxylation, which produces 8′-hydroxy-ABA (Cutler and Krochko, 1999). This compound isomerizes to phaseic acid (PA), which may be reduced to dihydrophaseic acid (DPA) (Okamoto et al., 2009). A minor oxidative route produces (+)-7′-hydroxy-ABA (7′OHABA), whereas a minor reductive pathway produces an unstable 1′,4′-diol ABA. ABA and its metabolites may also be conjugated with glucose to form ABA-β-D-glucosyl ester (ABA-GE) (Zaharia et al., 2005).

The enzyme 9-*cis*-epoxycarotenoid dioxygenase (NCED) catalyzes the rate-limiting step in ABA biosynthesis (Thompson et al., 2000). This gene encoding NCED form a small multigene family containing five members (*NCED2*, *3*, *5*, *6*, *9*) in *Arabidopsis thaliana* (Tan et al., 2003), and *NCED3* is mainly responsible for ABA accumulation under drought stress in *Arabidopsis* (Iuchi et al., 2001). *NCED3* has been demonstrated to act with *NCED5* against drought stress (Frey et al., 2012). Over-expression of *NCED* leading to ABA over-accumulation was first achieved in tomato and tobacco (Thompson et al., 2000); in tomato this increased root hydraulic conductivity and lowered g_s, resulting in higher water use efficiency (Thompson et al., 2007). In *Citrus*, when an *NCED3* ortholog, *CrNCED1*, was isolated from 'Cleopatra' mandarin (*Citrus reshni*) and overexpressed in transgenic tobacco, the plants showed higher levels of ABA and enhanced tolerance against drought, salt, and oxidative stresses when compared with WT (Xian et al., 2014). Although *NCED* genes have been well characterized in model plants under water deficiency (Xian et al., 2014), their responses in plants exposed to Al remain unknown.

As Al reduces g_s by a mechanism not yet elucidated, it is possible that Al toxicity alters *NCED* expression and the plant accumulates more ABA when compared to those not exposed to Al. Here we tested whether 1480 μM Al (40 mg L^{-1}), an Al concentration that reduces g_s in *Citrus* plants (Banhos et al., 2016; Cavalheiro et al., 2020), also up-regulates *NCED1*, *NCED3* and *NCED5*, and promotes ABA accumulation in roots and leaves of *C. limonia*. Furthermore, we sought to elucidate if ABA biosynthesis is induced before or after the reduction in leaf hydration, evidenced by low Ψ_w, RWC and g_s.

2. Material and methods

2.1. Plant material and experimental conditions

Seventy-two three-month-old and 15 ± 1 cm-high 'Rangpur' lime plants (*Citrus limonia* L.) were used for studying the plant hydration capacity when subjected to Al within a 90-day period. This species is an important rootstock for rain-fed *Citrus* plantations due to its high drought resistance (Banhos et al., 2016). At the beginning of the study, the plants had five leaves and were grown directly on an aerated nutrient solution inside opaque plastic boxes (50 cm in length x 30 cm in width x 15 cm in height; 20 L), with six plants per box, in a greenhouse.

The nutrient solution used was based on the solution proposed by Clark (1975), and it has been used to test Al tolerance in *C. limonia* (Banhos et al., 2016; Silva et al., 2018; Silva et al., 2019; Cavalheiro et al., 2020). It contained 1372.8 µM $Ca(NO_3)_2$, 507.0 µM NH_4NO_3, 224.4 µM KCl, 227.2 µM K_2SO_4, 218.6 µM KNO_3, 483.2 µM $Mg(NO_3)_2$, 12.9 µM KH_2PO_4, 26.0 µM $FeSO_4$, 23.8 µM NaEDTA, 3.5 µM $MnCl_2$, 9.9 µM H_3BO_3, 0.9 µM $ZnSO_4$, 0.2 µM $CuSO_4$ and 0.4 µM $NaMoO_2$. In previous studies we noted an Al-induced decrease in gas exchange rates when *C. limonia* was exposed to 1480 µM Al (40 mg L^{-1}) (Banhos et al., 2016; Silva et al., 2018; Cavalheiro et al., 2020). Therefore, the solution contained the aforementioned macro and micronutrients, as well as 0 and 1480 µM Al provided through $AlCl_3$. The nominal chemical composition of this solution was also tested on Geochem-EZ software (Shaff et al., 2010), resulting in more than 85% free Al^{3+} available. The pH of the solution was measured daily and maintained at 4.0 ± 0.1 (using NaOH and/or HCl) to guarantee Al solubility. The solution was totally replaced every 15 days, and the treatment with no added Al contained only trace amounts of Al.

Expanded polystyrene (Isopor®) 50 x 30 cm plates (2cm thick), with six holes (2.5 cm in diameter) each, were floated on the nutrient solution in the boxes, and the plants were fixed in these holes with polyurethane foam strips that were placed around the plant collar. The boxes with six plants each were randomly arranged on benches (80 cm above the ground) inside a greenhouse with semi-controlled conditions (air temperature 28.0 ± 2ºC; relative humidity 65.3 ± 2.5% — between 9h and 11:30h). The photoperiod of 13h of natural sunlight measured inside the greenhouse provided a photosynthetic photon flux density (PPFD) of 862.7 ± 184.4 µmol photons m^{-2} s^{-1}, between 9h and 11:30h.

2.2. Experimental design

After transplant, six boxes (36 plants) remained with the nutrient solution containing 0 µM Al and six other boxes (36 plants) received the nutrient solution containing 1480 µM Al. The plants grew in these conditions for 90 days, and non-destructive measurements (leaf gas exchange) and destructive measurements (leaf water potential (Ψ_w), relative leaf water content (RWC), NCED expression and ABA and its metabolites) were performed at 1, 7, 15, 30, 60 and 90 days after treatment (DAT). Using predawn (Ψ_{pd}) and midday (Ψ_{md}) leaf water potential and transpiration rates measured in the afternoon, we also estimated the hydraulic conductivity from roots to the leaves (K_L).

The excision of leaves for measuring Ψ_w, leaf discs for RWC and the collection of root tips for gene expression analysis were not performed on the same plants used for measuring leaf gas exchange, so that harmed plants did not interfere in the results of gas exchange rates. Leaf discs for RWC and the collection of leaf pieces and root tips were performed within 60 s, so that these variables interfered as little as possible in each other. In addition, the present study did not involve repeated measurements on the same plants through time, as one box (with 6 plants) per treatment was used on each evaluation date. The leaf pieces and root tips were collected, and their RNA was extracted for measuring NCED gene expression. Using six extra plants (0 DAT and 90 DAT), the biomass of leaves, stems, roots and the total plant biomass were assessed in order to check the severity of the Al treatment.

2.3. Analysis

2.3.1. Leaf gas exchange

CO_2 assimilation (A; µmol m^{-2} s^{-1}) and transpiration (E; mmol m^{-2} s^{-1}) rates, stomatal conductance (g_s; mol m^{-2} s^{-1}) and intercellular CO_2 (Ci; µmol mol^{-1}) were measured using an open gas exchange system (LI-6400xt; LI-COR, Lincoln, NE, USA). The water use efficiency ($WUE = A/E$) and intrinsic water use efficiency ($iWUE = A/gs$) were also calculated. The CO_2 concentration entering the leaf cuvette (LCF chamber; 2 cm^2, LI-COR) averaged 400 µmol mol^{-1}, as provided by the 6400-01 CO_2 mixer (LI-COR), as this was the air CO_2 concentration accepted for the experimental site when the study was performed. Measurements were taken between 9h and 11:30h on cloudless days, as it is the best period for measuring gas exchange parameters (Feistler and Habermann, 2012). We also measured gas exchange in the afternoon (13h-15h) in order to calculate the estimated hydraulic conductivity from roots to the leaves (K_L).

The PPFD in the leaf cuvette was provided by an artificial LED light source (6400-40 LCF, LI-COR), which was set to provide 90% red and 10% blue light at 1500 µmol photons m^{-2} s^{-1}, as this value saturates *A* for *C. limonia* as observed in *A*/*Ci* curves (Silva et al., 2018). The vapor pressure deficit (VPD) inside the leaf cuvette was similar to the external environment (inside the greenhouse), which was not higher than 1.5 kPa and relative humidity was approximately 65% on the days of measurement.

2.3.2. Water relations

Ψ_{pd} and Ψ_{md} (under maximum VPD) were measured (MPa) by the pressure chamber method (Turner, 1981), using a 3005F01 Plant Water Status Console (Soil Moisture, Santa Barbara, CA, USA) chamber.

The estimated hydraulic conductivity from roots to the leaves (K_L; mmol H_2O m^{-2} s^{-1} MPa^{-1}) was determined by the method proposed by Hubbard et al. (2001), which is based on Ohm's Law. For this, the following equation was applied:

$$K_L = E_{14h} / (\Psi_{pd} - \Psi_{md}),$$

where E_{14h} is the transpiration rate (*E*) measured between 13:00h and 15:00h under maximum VPD; Ψ_{pd} is assumed as the soil water potential (Ψ_{soil}), and Ψ_{md} is Ψw measured under maximum VPD. Although the plants were grown directly on nutrient solution, the $\Psi_{pd} = \Psi_{soil}$ principle is still accepted because Ψ_{pd} is measured before sunrise in non-transpiring plants and, therefore, Ψ_{pd} represents the plant's capacity to rehydrate overnight (Turner, 1981). This method was previously used for measuring K_L in *Citrus sinensis* (Magalhães Filho et al., 2009) and *C. limonia* (Cavalheiro et al., 2020) grown on nutrient solution.

For measuring RWC (%), leaf discs were collected at 13h-15h from plants of both treatments and calculated as:

$$RWC = [(FM-DM)/(TM-DM)] \times 100,$$

where FM is the fresh mass (immediately measured after collection); TM is the turgid mass, measured after rehydrating samples for 24 h in 100 mL deionized water inside amber flasks (to avoid photosynthetic activity); and DM is the dry mass, measured after oven-drying the discs at 60ºC for 48 h, according to Silva et al. (2018).

2.3.3. Gene expression analysis

Leaf pieces (≈ 1 cm^2) or root pieces (1 cm in length), totaling 100 mg (fresh mass) for each leaf or root sample (n = 4), were collected at 13h-15h, frozen in liquid nitrogen and stored

at -80ºC for future analysis. Total RNA was extracted from leaf and root samples using the RNeasy Plant Mini Kit (Qiagen, Hilden, Germany). Total RNA (2 µg) was treated with RNase-free TURBO DNase (Ambion, Carlsbad, USA) and reverse transcribed to cDNA using oligo-dT and the GoScript Reverse Transcription System kit (Promega Corp., Madison, WI, USA), according to the manufacturer's protocol (Life Technologies, Carlsbad, CA, USA). Gene expression analysis was carried out by quantitative real-time PCR (qRT-PCR) with SYBR green GoTaq q-PCR Master Mix (Promega Corp., USA), using Applied Biosystems QuantStudio 3 (Life Technologies, Carlsbad, CA, USA). The primers of *ClNCED1*, *ClNCED3* and *ClNCED5* (Table 1) used in the experiment were previously used in *Citrus* species (Agusti et al., 2007, Bassene et al., 2009), including *C. limonia* (Neves et al., 2013). As reference genes, we used glyceraldehyde-3-phosphate dehydrogenase (*GAPC2*) and elongation factor 1-alpha (*EFα*) (Table 1), which were proposed by Mafra et al. (2012) and used previously by Silva et al. (2019). Amplification efficiencies were calculated for each primer using Miner software (Zhao and Fernald, 2005).

For calculating the relative expression, Ct (cycle threshold) values of each sample, which were determined by the average of three technical replicates, were converted into relative quantities (RQ) according to Pfaffl (2001), using the following equation:

$$RQ=E^{\Delta Ct},$$

where E is the primer efficiency, and ΔCt is the difference between control Ct value for the evaluated gene and Ct value of the given sample. A normalization factor (NF) for each sample was calculated by the geometric mean of the RQ values of *GAPC2* and *EFα*. Normalized-relative quantity (NRQ) of each sample was calculated as the ratio of the sample RQ and the appropriate NF. Individual fold change values were determined by dividing the sample NRQ by mean values of NRQ that were obtained from the calibrator, i.e., root samples of plants not exposed to Al. Following this, fold change in the control group always shows a mean value of 1. Four independent biological replicates (plant samples) were used to calculate mean for each time point and treatment combination.

2.3.4. Quantification of ABA and metabolites

ABA and its metabolites, phaseic acid (PA), dihydrophaseic acid (DPA), (+)-7′-hydroxy-ABA (7′-OH ABA) and ABA-β-D-glucosyl ester (ABA-GE) were analyzed via liquid chromatography/tandem mass spectrophotometry (LC/MS-MS) on a SciexExionLC coupled with a QTRAP 6500+ mass spectrophotometer, following the method proposed by Morris et al. (2019).

Leaf and root samples (500 mg DM) were ground to a powder (in 2 mL micro-centrifuge tubes containing two 5 mm acid-rinsed glass balls) in a Star-Beater (VWR) at 30 Hz for 2 min. The powdered material, ~20 mg for leaf samples and ~50 mg for roots, with 1 ng of internal standards added, were extracted using a Star-Beater at 30 Hz for 2 min with 1 mL of ice-cold methanol/formic acid/water solvent (60:5:35 v/v). The internal standards used were: [$^2H_4$]-abscisic acid (-)-5,8′,8′,8′ (d_4-ABA); [$^2H_3$]-phaseic acid (-)-7′,7′,7′(d_3-PA); [$^2H_5$]-abscisic acid glucose ester (+)-4,5,8′,8′,8′ (d_5-ABA-GE); [$^2H_3$]-dihydrophaseic acid (-)-7′,7′,7′ (d_3-DPA); and [$^2H_4$]-7′-hydroxy-abscisic acid (±)-5,8′,8′,8′ (d_4-7OH-ABA). After extraction, the samples were left on ice in the dark for 20 min and, subsequently, the plant material was pelleted by centrifugation at 24,000 × g at 4˚C for 10 min. The supernatant was pipetted into 15 mL conical centrifuge tubes and the solvent was evaporated overnight in a freeze-drier (-105˚C; Scanvac, CoolSafe 110-4 Pro). Samples were reconstituted (vortexed for 2 min at 1400 rpm, sonicated for 30s and a final vortex at 2000 rpm for 3 min) in 1 mL of 5% acetonitrile in 10 mM ammonium formate (pH 3.4, adjusted with formic acid). Finally, the samples were filtered through 4 mm nylon filters (0.2 µM pore size, Whatman) into silanised amber HPLC vials.

Calibration samples consisted of a series of non-deuterated compounds (from 0.1 to 500 ng mL^{-1}), each with deuterated compounds (constant 1 ng mL^{-1}). Extracts and calibration samples (20 µL) were injected with an auto-sampler into a Luna 3 µm C18(2) 100 x 2 mm (Phenomenex) column with guard column at 30°C. The aqueous mobile phase (A) consisted of 2% acetonitrile in 10 mM ammonium formate, and the organic mobile phase (B) was 95% acetonitrile and 0.1% formic acid. The ratios of mobile phase A:B for separation of compounds was as follows (at a flow rate of 600 µL min^{-1}): 0-1.5 min at 96:4; 1.5-7 min at 87.4:12.6 and 7-10 min at 74:26. The column was then cleaned as follows, 10-10.5 min at 60:40; 10.5-10.6 min at 50:50 and 10.6-11.6 min at 0:100. The column was then equilibrated from 11.6-13 min at 96:4 before injection of the next sample. Analyst 1.6.3 and MultiQuant 3.0.2 (Sciex, Singapore) software was used for acquisition and quantification, respectively.

2.3.5. Biometric parameters

At 0 and 90 DAT, after separating the plant parts into leaves (plus petioles), stems and roots, the number of leaves was counted, and the shoot length was measured with a ruler. The total leaf area per plant (LA) was measured with an area meter (LI-3100C, LI-COR, USA). Total root length, root surface area and root diameter were measured using a scanner (Epson perfection v700 photo, Suwa, Japan), which was coupled to a computer running the

278 WinRHIZO^{TM} software (Regent Instruments, Canada). The biomass of organs was measured
279 on a 0.001g precision scale (AR2140, OHAUS, USA) after oven-drying the samples at 60°C
280 until constant mass.
281
282 **2.3.6. Aluminum quantification**
283 Dry samples of leaves and roots were sent to a plant nutrition laboratory at University
284 of São Paulo (ESALQ, USP, Piracicaba, Brazil) where these were ground and digested in a
285 solution of sulfuric:nitric:percloric acids (1:10:2, v/v/v). After digestion, Al concentrations
286 were determined by the atomic absorption spectrophotometer method (Sarruge and Haag,
287 1974) and expressed as mg Al per kg dry mass.
288
289 **2.3.7. Data analysis**
290 Leaf gas exchange parameters (*A*, g_s, *E*, *Ci*, *WUE* and *iWUE*), RWC and biomass of
291 organs were measured using six plant replicates. Leaf water potential (Ψ_{pd} and Ψ_{md}), estimation
292 of hydraulic conductivity from roots to the leaves (K_L), gene expression of NCED and ABA
293 metabolites were assessed using four plant replicates.
294 A student's t-test ($\propto = 0.05$) was used, separately for each evaluation date (1, 7, 15, 30,
295 60 and 90 DAT), to test differences between 0 and 1480 µM Al for each variable, as well as
296 when testing differences in plant biomass and Al concentration in plant organs between 0 and
297 90 DAT within each treatment.
298
299 **3. Results**
300 *3.1. Biometric parameters*
301 As expected, Al reduced the size of plants (Supplementary material; Fig. S1). At 90
302 DAT, Al significantly limited the main root length (-48%) (Fig. 1A), root surface area (-62%)
303 (Fig. 1B) and root biomass (-65%) (Fig. 1D), while the root diameter was enhanced in plants
304 exposed to Al (+25%) (Fig. 1C).
305 From 0 to 90 DAT, the leaf number (Fig. 2A), leaf area (Fig. 2B) and leaf biomass (Fig.
306 2C) increased by 31%, 83% and 59%, respectively, in plants exposed to Al and 140%, 504%
307 and 393%, respectively, in control plants. At 90 DAT, Al significantly decreased the leaf
308 number (-45%) (Fig. 2A), leaf area (-70%) (Fig. 2B) and leaf biomass (-68%) (Fig. 2C). Thus,
309 Al inhibited root growth, leaf initiation, leaf expansion and organ biomass accumulation, but
310 caused root thickening.

311

312 *3.2. Leaf gas exchange*

313 Compared to plants not exposed to Al, values of *A* (Fig. 3A), *gs* (Fig. 3B) and *E* (Fig.
314 3C) decreased from 7 DAT, and at 90 DAT these parameters were 71%, 78% and 60% lower
315 in plants exposed to Al. On the other hand, *Ci* values increased in plants exposed to Al from
316 15 DAT, being 55% higher at 90 DAT (Fig. 3D). The *WUE* was the same between the
317 treatments throughout the study (Fig. 3E), while *iWUE* was higher in plants exposed to Al from
318 30 DAT, being 108% higher at 90 DAT (Fig. 3F). This data is consistent with stomatal closure
319 leading to reductions of *A*. That is, a larger effect of Al toxicity on g_s than on *A* resulted in an
320 increase in A/g_s (*iWUE*).

321

322 *3.4. Water relations*

323 Ψ_{pd} was lower in plants exposed to Al throughout the study, although this was not
324 statistically significant (Fig. 4A). However, plants exposed to Al showed significantly lower
325 Ψ_{md} (Fig. 4B) and RWC (Fig. 5A) when compared to control plants from 7 DAT onwards. At
326 90 DAT, Al reduced Ψ_{md} from -1.2 to -2.2 (Fig. 4B) and RWC from 89% to 67% (Fig. 5A).
327 K_L was also lower in plants exposed to Al from 7 DAT, being 80% lower than control plants
328 at 90 DAT (Fig. 5B). Thus, Al compromised plant water status.

329

330 *3.5. NCED gene expression*

331 In the leaves, Al enhanced NCED genes expression over time (Fig. 6A, 6C and 6E),
332 while in the roots Al caused a peak for *ClNCED5* (Fig. 6F) and *ClNCED3* (Fig. 6D), most
333 pronounced in the latter. The Al-induced up-regulation of leaf *ClNCED3* started at 15 DAT,
334 being 78-fold higher at 90 DAT (Fig. 6C). For leaf *ClNCED1* and *ClNCED5*, significant up-
335 regulation occurred at 60 and 90 DAT, and on these dates up-regulation was of approximately
336 80- (Fig. 6A) and 35-fold higher (Fig. 6E) than the control, respectively. In the roots, Al caused
337 up-regulation of *ClNCED3* on all dates except for 7 DAT, reaching a peak of 16-fold higher
338 than control plants at 30 DAT (Fig. 6D). Root *ClNCED5* was significantly up-regulated by Al
339 (4-fold higher) only at 60 DAT, while no up-regulation in root *ClNCED1* was induced by Al
340 (Fig. 6B). Thus, Al up-regulated the key genes of ABA biosynthesis (*ClNCED3*) in the roots
341 at 1 DAT (Fig. 6D), while decreases in leaf hydration were detected at 7 DAT for g_s (Fig. 3B),
342 Ψ_{md} (Fig. 4B), RWC (Fig. 5A) and K_L (Fig. 5B).

343

344 *3.6. Abscisic acid (ABA) accumulation in leaves and roots*

345 In general, Al increased ABA concentrations in leaves and roots (Fig. 7A, 7B). In plants
346 exposed to Al, $[ABA]_{leaf}$ increased from 7 DAT, being 4.7-times higher than the control at 90
347 DAT (Fig. 7A). $[DPA]_{leaf}$ and $[7'OH\ ABA]_{leaf}$ increased in plants exposed to Al from 15 DAT,
348 being 1.3- and 1.5-times higher than the control, respectively, over this period (Fig. 7E, 7G).
349 $[PA]_{leaf}$ and $[ABA\text{-}GE]_{leaf}$, however, were higher in plants exposed to Al only at 90 DAT, being
350 2.6- and 2.0-times higher, respectively, when compared to the control (7C, 7I). Therefore, Al
351 caused a consistent increase in [ABA], [DPA] and [7′OH ABA] from the first week of the
352 study, while [PA] and [ABA-GE] increased only after 90 days of Al exposure.

353 In the roots, Al caused a peak of $[ABA]_{root}$ (3-times higher than the control; Fig. 7B),
354 $[PA]_{root}$ (7-times higher; Fig. 7D) and $[ABA\text{-}GE]_{root}$ (3.3-times higher; Fig. 7J) at 7, 1 and 30
355 DAT, respectively. After these peaks, the concentration of these metabolites in the roots
356 decreased, but remained higher in plants exposed to Al at 15 and 30 DAT (ABA; Fig. 7B), 30
357 and 60 DAT (PA; Fig. 7D) and until 90 DAT (ABA-GE; Fig. 7J). $[DPA]_{root}$ of plants exposed
358 to Al was 2.0-times higher than control plants only at 90 DAT (Fig. 7F), while $[7'OH\ ABA]_{root}$
359 showed no pattern, with variable values between treatments (Fig. 7H).

360 Thus, Al increased ABA in the roots immediately after Al exposure and, in the leaves,
361 Al induced a consistent accumulation, especially for ABA, DPA and 7′OH ABA. In the leaves
362 of plants exposed to Al, ABA accumulation seems to be associated with *ClNCED3*
363 (Supplementary material; Fig. S2). In addition, in Al-treated plants, $[ABA]_{leaf}$ is driving major
364 part of g_s responses (Supplementary material; Fig. S3), which also corroborates low values of
365 RWC, Ψ_{md} and K_L of plants exposed to Al.

366

367 *3.7. Aluminum retention in plant organs*

368 As expected, Al concentration in the roots was approximately 10 times higher than the
369 leaves of plants exposed to Al (Fig. 8). From 0 to 90 DAT, leaf and root Al concentration
370 increased by seven- (Fig. 8A) and 15-times (Fig. 8B), respectively, in control plants when
371 compared to those treated with Al.

372

373 **4. Discussion**

374 Hydraulic signals, in the form of turgor changes in the leaves, and hormonal signaling
375 have been proposed to control g_s (McAdam and Brodribb, 2015; Huber et al., 2019). Plant
376 hormones can influence the Al toxicity and development of symptoms (Kopittke, 2016), as
377 well as these compounds can mediate the Al resistance, especially in the root environment

(Massot et al., 2002; Yang et al., 2017). The well-known role of ABA in causing stomatal closure, the up regulation of ABA biosynthesis upon changes in cell turgor and water availability (McAdam et al., 2016; Sussmilch et al., 2017; Zhang et al., 2018) makes ABA a candidate for causing the decrease in g_s during Al toxicity. In the present study, we tested whether ABA accumulation in roots and leaves could be responsible for the Al-induced low g_s usually found in *Citrus limonia* exposed to Al (Banhos et al., 2016; Silva et al., 2018; Cavalheiro et al., 2020).

4.1. Effect of Al on plant water relations

Our results show that *A* and *E* were progressively reduced in plants exposed to Al (Fig. 3A and 3C), and these reductions could be explained by the low g_s values (Fig. 3B). In our previous studies with this same species under the same Al concentration, low *A* values were largely explained by low g_s rather than decreased photochemical performance (Banhos et al., 2016; Silva et al, 2018). In addition, Al-induced reduction in g_s has been observed in other *Citrus* plants, including 'Cleopatra' tangerine (-30%; Chen et al., 2005b) and 'Sour Pummelo' (-40%; Jiang et al., 2008). Therefore, the decrease in g_s seems to be a key response in plants exposed to Al.

Plants adjust their xylem pressure with concomitant stomatal regulation (Creek et al., 2020; Rodriguez-Dominguez and Brodribb, 2019). In the present study, the decrease in g_s of plants exposed to Al was not sufficient to maintain the leaf water status, as evidenced by low values of Ψ_{md} (Fig. 4B) and RWC (Fig. 5A) from 7 DAT. K_L represents the plant capacity to supply water to the mesophyll (Rodríguez-Gamir et al., 2019) and since its value dropped by 80% under Al toxicity (Fig. 5B), the ability of the Al-treated plants to transport water to the leaves was dramatically impaired. Indeed, root hydraulic conductance (Lp_r) of *Solanum lycopersicum* (tomato) also declined proportionally to the increase of Al in nutrient solution (Gavassi et al., 2020). Reductions in K_L and low expression of aquaporins (PIP family) in *C. limonia* exposed to 1480 µM Al found by Cavalheiro et al. (2020) have been associated with fibrous xylem vessels (Banhos et al., 2016) and more lignin deposition in the vascular cylinder (Silva et al., 2019) of *C. limonia* grown under the same Al toxicity conditions. The root apex senses Al toxicity (Ryan et al., 1993; Horst et al., 2010), and, despite being anatomically "disconnected" from the xylem, the longer the exposure of root tips of *C. limonia* to Al, the more lignin deposition is found in their vascular cylinders (Silva et al., 2019), although the mechanism(s) of signaling between Al perception and xylem damage is unclear. The vascular cylinder was also the most affected part of the root of maize plants, and their proto- and

412 metaxylem did not reach full maturation under 300 μM Al (Batista et al., 2013). In addition,
413 ten-times more Al was found in root tips (1 cm long) of maize plants exposed to 50 μM Al
414 when compared to plants not exposed to Al after 24h (Souza et al., 2016). This same proportion
415 was found in the roots of plants exposed to Al when compared to control plants, at 90 DAT
416 (Fig. 8B). Furthermore, once Al is firmly bound to a root cell wall, where it is the site of
417 primary lesion (Kopittke et al., 2015), it does not seem to be released (Rangel et al., 2009), and
418 it could cause anatomical damage to the cortex and xylem of plant roots, as observed by Batista
419 et al. (2013), Banhos et al. (2016) and Silva et al. (2019). Taken together, these results suggest
420 that Al impairs the plant capacity to transport water to the leaves. A key question, however, is
421 whether the impairment of root and vascular function leads directly to declining shoot water
422 status and productivity (reduced g_s, A and biomass), or whether this is controlled by early
423 hormonal signals.
424
425 *4.2. The role of ABA and its metabolites in short-term responses*
426 In the present study, root ABA increased at 1 DAT (Fig. 7B) relative to control, prior
427 to any significant decreases in Ψ_{pd}, Ψ_{md}, RWC or K_L (Fig. 4 and 5); and ABA kept increasing
428 in the root until 7 DAT (Fig. 7B). PA concentration was also higher at 1 DAT, compared to
429 control plants (Fig. 7D); this could also contribute to physiological responses because PA
430 showed biological activity *in vitro*, activating members of the ABA receptor family, albeit with
431 a lower affinity than ABA (Weng et al. 2016). Although not presenting biological activity,
432 ABA-GE was higher in the roots of plants exposed to Al on all dates, including 1 DAT,
433 although showing a peak at 30 DAT (Fig 7J). ABA-GE is considered an ABA metabolite and
434 can be transported symplastically from the cytosol of root cells to xylem parenchyma cells and
435 be released to xylem vessels (Priest et al., 2006) as a root-to-shoot signal (Sauter et al., 2002).
436 Therefore, the extra ABA-GE produced from 1 DAT in the Al-treated roots could have been
437 transported, de-glycosylated and have contributed to the ABA level and stomatal closure at 7
438 DAT. Analysis of gene expression in the early period 1-7 DAT indicated that *ClNCED3*
439 responded to the Al treatment in the roots, but the increase was small (Fig. 6D). This small
440 increase could have contributed to the rise in ABA, PA and ABA-GE. Alternatively, an
441 activation of NCED enzyme activity at the protein level, or a change in transport processes
442 between root and shoot might explain the early spike in ABA given that there was only a small
443 increase in *ClNCED3* gene expression. Furthermore, the catabolic product PA increased at 1

DAT (Fig. 7D), suggesting that slower ABA catabolism was not the reason for ABA accumulation in the roots of Al-treated plants.

Overall, the very early rise in root ABA, PA and ABA-GE caused by Al toxicity appeared to precede the decline in g_s, and so is potentially the cause of stomatal closure. However, this reduction in g_s, preventing water loss, was not able to stop a decline in leaf water status, presumably caused by the impact of Al on root water transport function as suggested by Batista et al. (2013), Banhos et al. (2016), Silva et al. (2019), Cavalheiro et al. (2020) and Gavassi et al. (2020), and also supported by the 80% lower K_L in plants exposed to Al (Fig. 5B). The coincident reduction in g_s and shoot water status at 7 DAT means that we cannot exclude a hydraulic signal as the cause of stomatal closure.

4.3. The role of ABA and metabolites in longer-term responses

In the leaves of plants exposed to Al, ABA progressively increased until the end of the study (Fig. 7A) with the first significant increase occurring at 7 DAT. This was accompanied by similar trends of DPA from 15 DAT (Fig. 7E), but surprisingly $[DPA]_{leaf}$ peaked 25-fold higher in absolute concentration than $[ABA]_{leaf}$, suggesting a high rate of catabolism to DPA that has previously been observed in *Citrus* leaves under drought and soil flooding stresses (Jitratham et al., 2006; Arbona et al., 2017). ABA accumulation in the leaf occurred later and more progressively than in the root, and after, or co-incident with, the decline in water relations (RWC, Ψ_{md} and K_L all down at 7 DAT). Therefore the leaf ABA and PA was likely increased as a secondary consequence of the Al toxicity, where lack of water supply to the shoot (low K_L) led to reduced shoot water status which then stimulated accumulation of ABA and PA and reinforced stomatal closure: in plants exposed to Al, $[ABA]_{leaf}$ was inversely correlated with *gs* values (Supplementary material; Fig. S3).

The expression of genes encoding NCED did not fully explain the increase in ABA and DPA in the leaf. The first increase was for *ClNCED3* at 15 DAT, after the rise in ABA, and this initial increase for *ClNCED3* was small (2-fold), with the peak occurring at 90 DAT (Fig. 6C). However, the linear correlation (R^2) between *ClNCED3* and $[ABA]_{leaf}$ in plants exposed to Al was 0.875 (Supplementary material; Fig. S2). This suggests that progressive increase in $[ABA]_{leaf}$ may be explained by *ClNCED3* expression. In the leaf, *ClNCED1* and *ClNCED5* also showed up-regulation of approximately 80- and 30-fold higher than control plants, respectively, at 60 and 90 DAT (Fig. 6A and 6E), but this rise was even later than for *ClNCED3*; therefore it did not explain the initial increase in ABA from 7 DAT in the leaf, but may have contributed to the continued and accelerated increase in ABA and PA which showed

a sharp rise between 60 and 90 DAT. The increase in *ClNCED3* expression from 15 DAT, and of *ClNCED1* and *ClNCED5* from 60 DAT, was probably driven by reduced cellular water status in the leaf since orthologs of this gene are known to respond in this way. In *Arabidopsis*, the orthologous *AtNCED3* is predominantly induced by drought and controls endogenous ABA content in this condition (Endo et al., 2008; Hao et al., 2009), but *AtNCED5* and *AtNCED3* participate together in water deficit response (Frey et al., 2012). In *Citrus*, *NCED1* was up-regulated by drought in leaves of *C. sinensis* (Rodrigo et al., 2006; Xian et al., 2014) and *C. reshni* (Zandalinas et al., 2016), as also observed here in the leaves of plants exposed to Al (Fig. 6A). Up-regulation of *ClNCED5* was previously observed in leaves of *C. limonia* submitted to 40 days of drought (Neves et al., 2013).

Thus, only the later, but not the early increase in ABA and DPA, could be explained by *NCED* gene expression in the leaves; other mechanisms, such as reduced catabolism, post-transcriptional control or redistribution of ABA would need to be invoked.

4.4. Impact of reduced growth rate on physiological responses

Critics could still argue that the conspicuous decrease in root growth parameters caused by Al at 90 DAT (Fig. 1A, 1B and 1D) could have acted as a physical limitation for water uptake, which could not maintain leaf transpiration, explaining the low g_s values. However, this low root growth was followed by reduced leaf number (Fig. 2A), leaf area (Fig. 2B) and leaf biomass (Fig. 2C), which would have greatly reduced the demand for water transport from the smaller root system. Similarly, tomato plants exposed to 0, 25 and 50 μM Al showed similar root/leaf area ratio, reinforcing that the decrease in the root size is compensated by a low shoot growth (Gavassi et al., 2020).

We have measured biometric parameters only at 90 DAT, but it seems unlikely that reduced root growth could have occurred at 7 DAT and have caused low g_s values due to fewer roots responsible for (less) water uptake. Further evidence in this regard deserves investigation.

5. Conclusions

We showed that Al triggered *ClNCED3* expression and ABA biosynthesis in the roots 1 day after Al exposure in *C. limonia*, before impairments in leaf hydration (low Ψw, RWC and g_s) could be observed. In addition, leaf ABA concentration increased from 7 to 90 DAT and this could be partially explained by the increased expression of *ClNCED3*, *ClNCED1* and *ClNCED5* in this organ. Stomatal closure occurred concomitantly with the increase of ABA

concentration and this result provides further evidence of the role of ABA modulation of plant hydration under Al stress.

Acknowledgements

We thank the Sanicitrus Nursery (Araras, São Paulo state, Brazil) for providing us with the *C. limonia* plants.

Funding sources

This work was supported by the São Paulo Research Foundation (Fapesp) [grant numbers 2015/25409-4, 2018/08902-7, 2018/25658-2, 2017/26144-0] and the Brazilian National Council for Scientific and Technological Development (CNPq) [grant number 141342/2016-1, 309149/2017-7].

References

Agusti, J., Zapater, M., Iglesias, D.J., Cercós, M., Tadeo, F.R., Talón, M., 2007. Differential expression of putative 9-cis epoxycarotenoid dioxygenases and abscisic acid accumulation in water stressed vegetative and reproductive tissues of citrus. Plant Sci. 172, 85–94.

Ali, S., Zeng, F., Qiu, L., Zhang, G. 2011. The effect of chromium and aluminum on growth, root morphology, photosynthetic parameters and transpiration of the two barley cultivars. Biol. Plant. 55, 291-296.

Anjum, A.S., Ashraf, U., Khan, I., Tanveer, M., Saleem, M.F., Wang, L. 2016. Aluminum and chromium toxicity in maize: implications for agronomic attributes, net photosynthesis, physio-biochemical oscillations, and metal accumulation in different plant parts. Water Air Soil Pollut. 227, 326.

Arbona, V., Zandalinas, S.I., Manzi, M., González-Guzmán, M., Rodriguez, P.L., Gómez-Cadenas, A., 2017. Depletion of abscisic acid levels in roots of flooded Carrizo citrange (*Poncirus trifoliata* L. Raf. × *Citrus sinensis* L. Osb.) plants is a stress-specific response associated to the differential expression of PYR/PYL/RCAR receptors. Plant Mol. Biol. 93, 623-640.

Banhos, O.F.A.A., Carvalho, B.M.O., Veiga, E.B., Bressan, A.C.G., Tanaka, F.A.O., Habermann, G., 2016. Aluminum-induced decrease in CO_2 assimilation in 'Rangpur' lime is associated with low stomatal conductance rather than low photochemical performances. Sci. Hortic. 205, 133-140.

Bassene, J.B., Froelicher, Y., Dhuique-Mayer, C.M., Mouhaya, W., Ferrer, R.M., Ancillo, G., Morillon, R., Navarro, L., Ollitraaut, P., 2009. Nonadditive phenotypic and transcriptomic inheritance in a citrus allotetraploid somatic hybrid between *C. reticulata* and *C. limon*: the case of pulp carotenoid biosynthesis pathway. Plant Cell Rep. 28, 1689–1697.

Batista, M.F., Moscheta, I.S., Bonato, C.M., Batista, M.A., Almeida, O.J.G., Inoue, T.T., 2013. Aluminum in corn plants: influence on growth and morpho-anatomy of root and leaf. Rev Bras Cienc Solo 37, 177-187.

Cavalheiro, M.F., Gavassi, M.A., Silva, G.S., Nogueira, M.A., Silva, C.M.S., Domingues, D.S., Habermann, G., 2020. Low root PIP1-1 and PIP2 aquaporins expression could be related to reduced hydration in 'Rangpur' lime plants exposed to aluminum. Funct. Plant Biol. 47, 112-121.

Clark, R.B., 1975. Characterization of phosphatase of intact maize roots. J. Agric. Food Chem. 23, 458–460.

Chen, L-S., QI, Y.-P., Smith, B.R., Liu, X.H., 2005. Aluminum-induced decrease in CO_2 assimilation in citrus seedlings is unaccompanied by decreased activities of key enzymes involved in CO_2 assimilation. Tree Physiol. 25, 317–324.

Creek, D., Lamarque, L.J., Torres-Ruiz, J.M., Parise, C., Burlett, R., Tissue, D.T., Delzon, S., 2020. Xylem embolism in leaves does not occur with open stomata: evidence from direct observations using the optical visualization technique. J. Exp. Bot. 71, 1151-1159.

Cutler, A.J., Krochko, J.E., 1999. Formation and breakdown of ABA. Trends Plant Sci. 4, 472–478

Dodd, I.C., 2003. Leaf area development of ABA-deficient and wildtype peas at two levels of nitrogen supply. Funct. Plant Biol. 30, 777–783.

Endo, A., Sawada, Y., Takahashi, H., Okamoto, M., Ikegami, K., Koiwai, H., Seo, M., Toyomasu, T., Mitsuhashi, W., Shinozaki, K., Nakazono, M., Kamiya, Y., Koshiba, T., Nambara, E., 2008. Drought induction of Arabidopsis 9-cis-epoxycarotenoid dioxygenase occurs in vascular parenchyma cells. Plant Physiol. 147, 1984–1993.

Estrada-Melo, A.C., Reid, M.S., Jiang, C.Z., 2015. Overexpression of an ABA biosynthesis gene using a stress-inducible promoter enhances drought resistance in petunia. Hort. Res. 2, 15013.

Feistler, A.M., Habermann, G., 2012. Assessing the role of vertical leaves within the photosynthetic function of *Styax camporum* under drought conditions. Photosynthetica 50, 613-622.

Frey, A., Effroy, D., Lefebvre, V., Seo, M., Perreau, F., Berger, A., Sechet, J., To, A., North, H.M., Marion-Poll, A., 2012. Epoxycarotenoid cleavage by NCED5 fine-tunes ABA accumulation and affects seed dormancy and drought tolerance with other NCED family members. Plant J 70, 501–512.

Gavassi, M.A., Dodd, I.C., Puértolas, J., Silva, G.S., Carvalho, R.F., Habermann, G., 2020. Aluminum-induced stomatal closure is related to low root hydraulic conductance and high ABA accumulation. Env. Exp. Bot. *in press.* doi: https://doi.org/10.1016/j.envexpbot.2020.104233

Gunsé, B., Poschenrieder, C., Barceló, J., 1997. Water transport properties of roots and root cortical cells in proton- and Al-stressed maize varieties. Plant Physiol. 113, 595–602.

Hao, G.P., Zhang, X.H., Wang, Y.Q., Wu, Z.Y., Huang, C.L., 2009. Nucleotide variation in the NCED3 region of *Arabidopsis thaliana* and its association study with abscisic acid content under drought stress. J Integr Plant Biol 51, 175–183.

Horst, W.J., Wang, Y., Eticha, D. 2010. The role of the root apoplast in aluminium-induced inhibition of root elongation and in aluminium resistance of plants: a review. Ann. Bot. 106, 187–197.

Hou, N., You, J., Pang, J., Xu, M., Chen, G., Yang, Z., 2010. The accumulation and transport of abscisic acid in soybean (*Glycine max* L.) under aluminum stress. Plant Soil 330, 127–137.

Hubbard, R.M., Ryan, M.G., Stiller, V., Sperry, J.S. 2001. Stomatal conductance and photosynthesis vary linearly with plant hydraulic conductance in ponderosa pine. Plant Cell Environ. 24, 113–121.

Huber, A.E., Melcher, P.J., Piñeros, M.A., Setter, T.L., Baueler, TL., 2019. Signal coordination before, during and after stomatal closure in response to drought stress. New Phytol. 224, 675–688.

Iuchi, S., Kobayashi, M., Taji, T., Naramoto, M., Seki, M., Kato, T., Tabata, S., Kakubari, Y., Yamaguchi-Shinozaki, K., Shinozaki, K., 2001. Regulation of drought tolerance by gene manipulation of 9-cisepoxycarotenoid dioxygenase, a key enzyme in abscisic acid biosynthesis in Arabidopsis. Plant J. 27, 325–333.

Jiang, H-X., Chen, L-S., Zheng, J-G., Han, S., Tang, N., Smith, B.R., 2008. Aluminum-induced effects on Photosystem II photochemistry in Citrus leaves assessed by the chlorophyll a fluorescence transient. Tree Physiol. 28, 1863–1871.

Jitratham, A., Yazama, F., Kondo, S., 2006. Effects of drought stress on abscisic acid and jasmonate metabolism in *Citrus*. Environ. Control Biol. 44, 41-49.

Kopittke, P.M., Blamey, F.P.C., Menzies, N.W., 2008. Toxicities of Al, Cu, and La include ruptures to rhizodermal and root cortical cells of cowpea. Plant Soil 303, 217-227.

Kopittke, P.M, Moore, K.L., Lombi, E., Gianoncelli, A., Ferguson, B.J., Blamey, F.P.C., Menzies, N.W., Nicholson, T.M., McKenna, B.A., Wang, P., Gresshoff, P.M., Kourousias, G., Webb, R.I.,

Green, K., Tollenaere, A., 2015. Identification of the primary lesion of toxic aluminum in plant roots. Plant Physiol. 167, 1402-1411.

Kopittke, P.M., 2016. Role of phytohormones in aluminium rhizotoxicity. Plant Cell Environ. 39, 2319-2328.

Ma, Y., Cao, J., He, J., Chen, Q., Li, X., Yang, Y., 2018. Molecular Mechanism for the Regulation of ABA Homeostasis During Plant Development and Stress Responses. Int. J. Mol. Sci. 19, 3643.

Mafra, V., Kubo, K.S., Alves-Ferreira, M., Ribeiro-Alves, M., Stuart, R.M., Boava, L.P., Rodrigues, C.M., Machado, M.A., 2012. Reference genes for accurate transcript normalization in citrus genotypes under different experimental conditions. PloS ONE 7, e31263.

Magalhães Filho, J.R., Machado, E.C., Machado, D.F.S.P., Ramos, R.A., Ribeiro, R.V., 2009. Variação da temperatura do substrato e fotossíntese em mudas de laranjeira 'Valência'. Pesq. Agropec. Bras. 44, 1118–1126.

Massot, N., Nicander, B., Barceló, J., Poschenrieder, C., Tillberg, E., 2002. A rapid increase in cytokinin levels and enhanced ethylene evolution precede Al^{3+}-induced inhibition of root growth in bean seedlings (*Phaseolus vulgaris* L.). Plant Growth Regul. 37, 105–112.

McAdam, S.A.M., Brodribb T.J., 2015. The evolution of mechanisms driving the stomatal response to vapor pressure deficit. Plant Physiol. 167, 833–843.

McAdam, S.A.M., Sussmilch, F.C., Brodribb, T.J., 2016. Stomatal responses to vapour pressure deficit are regulated by high speed gene expression in angiosperms. Plant Cell Environ. 39, 485–491.

Merilo, E., Jalakas, P., Laanemets, K., Mohammadi, O., Hõrak, H., Kollist, H., Brosche, M., 2015. Abscisic acid transport and homeostasis in the context of stomatal regulation. Mol. Plant 8, 1321-1333.

Mehrotra, R., Bhalothia, P., Bansal, P., Basantani, M.K., Bharti., V., Mehrotra S., 2014. Abscisic acid and abiotic stress tolerance – Different tiers of regulation. Plant Physiol. 171, 486-496.

Morris, W.L., Alamar, M.C., Lopez-Cobollo, R.M., Castillo, J.C., Bennett, M., Van der Kaay, J., Stevens, J., Sharma, S.K., McLean, K., Thompson, M.J., Terry, L.A., Turnbull, C.G.N., Bryan, G.J., Taylor, MA., 2019. A member of the TERMINAL FLOWER 1/CENTRORADIALIS gene family controls sprout growth in potato tubers. J. Exp. Bot. 70, 835–843.

Neves, D.M., Coelho Filho, M.A., Bellete, B.S., Silva, M.F.G.F., Souza, D.T., Soares Filho, W.S., Costa, M.G.C., Gesteira, A.S., 2013. Comparative study of putative 9-cis-epoxycarotenoid dioxygenase and abscisic acid accumulation in the responses of Sunki mandarin and Rangpur lime to water deficit. Mol. Biol. Rep. 40, 5339–5349.

Ng, L.M., Melcher, K., The, B.T., Xu, H.E., 2014. Abscisic acid perception and signaling: structural mechanisms and applications. Acta Pharm. Sin. 35, 567–584.

Okamoto, M., Tanaka Y., Abrams S.R., Kamiya Y., Seki M., Nambara E., 2009. High humidity induces abscisic acid 8'-hydroxylase in stomata and vasculature to regulate local and systemic abscisic acid responses in *Arabidopsis*. Plant Physiol. 149, 825–834.

Panda, S.K., Baluska, F., Matsumoto, H., 2009. Aluminum stress signaling in plants. Plant Signal. Behav. 4, 592-597.

Pfaffl, M.W., 2001. A new mathematical model for relative quantification in real-time RT PCR. Nucleic

Acids Res. 29, 45–45.

Priest, D.M., Ambrose, S.J., Vaistij, F.E., Elias, L., Higgins, G.S., Ross, A.R., Abrams, S.R., Bowles, D.J., 2006. Use of the glucosyltransferase UGT71B6 to disturb abscisic acid homeostasis in *Arabidopsis thaliana*. Plant J. 46, 492–502.

Rangel, A.F., Rao, I.M., Horst, W.J., 2009. Intracellular distributing and biding state of aluminum in root apices of two common bean (*Phaseolus vulgaris*) genotypes in relation to Al toxicity. Physiol. Plant. 135, 162–173.

Reyna-Llorens, I., Corrales, I., Poschenrieder, C., Barcelo, J., Cruz-Ortega, R., 2015. Both aluminum and ABA induce the expression of an ABC-like transporter gene (FeALS3) in the Al-tolerant species *Fagopyrum esculentum*. Env. Exp. Bot. 111, 74–82.

Rodrigo, M.J., Alquezar,, B., Zacarías L., 2006. Cloning and characterization of two 9-*cis*-epoxycarotenoid dioxygenase genes, differentially regulated during fruit maturation and under stress conditions, from orange (*Citrus sinensis* L. Osbeck). J. Exp. Bot. 57, 633–643.

Rodriguez-Dominguez, C.M., Brodribb, T.J., 2019. Declining root water transport drives stomatal closure in olive under moderate water stress. New Phytol. 225, 126-134.

Rodríguez-Gamir, J., Xue, J., Clearwater, M.J., Meason, D.F., Clinton, P.W., Domec, J-C., 2019. Aquaporin regulation in roots controls plant hydraulic conductance, stomatal conductance, and leaf water potential in Pinus radiate under water stress. Plant Cell Environ. 42, 717-729.

Ryan, P.R., Ditomaso, J.M., Kochian, L.V., 1993. Aluminium toxicity in roots: an investigation of spatial sensitivity and the role of the root cap. J Exp Bot. 44, 437–446.

Sarruge, J.R., Haag, H.P., 1974. Análises químicas em plantas. Piracicaba, ESALQ.

Sauter, A., Dietz K.-J., Hartung, W., 2002. A possible stress physiological role of abscisic acid conjugates in root-to-shoot signalling. Plant Cell Environ. 25, 223–228.

Shaff, J.E., Shultz, B.A., Craft, E.J., Clark, R.T., Kochian, L.V., 2010. GEOCHEM-EZ: A chemical speciation program with greater power and flexibility. Plant Soil 330, 207–214.

Shen, H., Ligaba, A., Yamaguchi, M., Osawa, H., Shibata, K., Yan, X., Matsumoto H., 2004. Effect of K-252a and abscisic acid on the eflfux of citrate from soybean roots. J Exp Bot. 55, 663-671.

Silva, S., Pinto, G., Dias, M.C., Correira, C.M., Moutinho-Pereira, J., Pinto-Carnide, O., Santos, C., 2012. Aluminum long-term stress differently affects photossyntesis in rye genotypes. Plant Physiol. Biochem. 54, 105-112.

Silva, G.S., Gavassi, M.A., Nogueira, M.A., Habermann, G., 2018. Aluminum prevents stomatal conductance from responding to vapor pressure deficit in *Citrus limonia*. Environ. Exp. Bot. 155, 662–671.

Silva, C.M.S., Cavalheiro, M.F., Bressan, A.C.G., Carvalho, B.M.O., Banhos, O.F.A.A., Purgatto, E., Harakava, R., Tanaka, F.A.O., Habermann, G., 2019. Aluminum-induced high IAA concentration may explain the Al susceptibility in *Citrus limonia*. Plant Growth Regul. 87, 123–137.

Simon, L., Kieger, M., Sung, S.S., Smalley, T.J., 1994. Aluminum toxicity in tomato. Part 2. Leaf gas exchange, chlorophyll content, and invertase activity. J Plant Nutr. 17, 307–317.

Singh, S., Tripathi, D.K., Singh, S., Sharma, S., Dubey, N.K., Chauhan, D.K., Vaculík, M., 2017.

Toxicity of aluminium on various levels of plant cells and organism: A review. Environ. Exp. Bot. 137, 177–193.

Souza, T., Cambraia, J., Ribeiro, C., Oliveira, J.Á., Silva, L.C., 2016. Effects of aluminum on the elongation and external morphology of root tips in two maize genotypes. Bragantia 75, 19-25.

Sussmilch, F.C., Brodribb, T.J., McAdam, SAM., 2017. Up-regulation of NCED3 and ABA biosynthesis occur within minutes of a decrease in leaf turgor but AHK1 is not required. J. Exp. Bot. 68, 2913–2918.

Szatanik-Kloc, A., 2016. Changes in the size of the apparent surface area and adsorption energy of the rye roots by low pH and the presence of aluminum ions induced. Int Agrophs. 30, 375-381.

Tamás, L., Huttová, J., Mistrik, I., Simonovicová, M., Siroká, B., 2006. Aluminium-induced drought and oxidative stress in barley roots. J. Plant Physiol. 163, 781-784.

Tan, B-C., Joseph, L.M., Deng, W-T., Liu, L., Li, Q-B., Cline, K., McCarty, D.R., 2003. Molecular characterization of the *Arabidopsis* 9-*cis* epoxycarotenoid dioxygenase gene family. Plant J. 35, 44-56.

Thompson, A.J., Jackson, A.C., Symonds, R.C., Mulholland, B.J., Dadswell, A.R., Blake, P.S., Burbidge, A., Taylor I.B., 2000. Ectopic expression of a tomato 9-cis-epoxycarotenoid dioxygenase gene causes over-production of abscisic acid. Plant J. 23, 363–374.

Thompson, A.J., Andrews, J., Mulholland, B.J., McKee, J.M.T., Hilton, H.W., Horridge, J.S., Farquhar, G.D., Smeeton, R.C., Smillie, I.R.A., Black, C.R., Taylor, I.B., 2007. Overproduction of abscisic acid in tomato increases transpiration efficiency and root hydraulic conductivity and influences leaf expansion. Plant Physiol. 143, 1905–1917.

Turner N.C., 1981. Techniques and experimental approaches for the measurement of plant water status. Plant Soil 58, 339–366.

Vitorello, V.A., Capaldi, F.R., Stefanuto, V.A., 2005. Recent advances in aluminium toxicity and resistance in higher plants. Braz. J. Plant Physiol. 17, 129–143.

Weng, J.K., Ye, M., Li, B., Noel, J.P., 2016. Co-evolution of hormone metabolism and signaling networks expands plant adaptive plasticity. Cell 166, 881-893.

Xian, L., Sun, P., Hu, S., Wu, J., Liu, J-H., 2014. Molecular cloning and characterization of *CrNCED1*, a gene encoding 9-*cis*-epoxycarotenoid dioxygenase in *Citrus reshni*, with functions in tolerance to multiple abiotic stresses. Planta 239, 61-77.

Xiong, L., Zhu J., 2003. Regulation of Abscisic Acid Biosynthesis. Plant Physiol. 133, 29–36.

Xu, Z-Y., Kim, D.H., Hwang, I., 2013. ABA homeostasis and signaling involving multiple subcellular compartments and multiple receptors. Plant Cell Rep. 32, 807–813.

Yang, Z., Rao, I.M., Horst, W.J., 2013. Interaction of aluminium and drought stress on root growth and crop yield on acid soils. Plant Soil 372, 3–25.

Yang, Z-B., Liu, G., Liu, J., Zhang, B., Meng, W., Müller, B., Hayashi, K-i., Zhang, X., Zhao, Z., De Smet, I., Ding, Z., 2017. Synergistic action of auxin and cytokinin mediates aluminum-induced root growth inhibition in *Arabidopsis*. EMBO Rep. 7, 1213-1230.

Zaharia, L.I., Walker-Simmon, M.K., Rodrígues, C.N., Abrams, S.R., 2005. Chemistry of abscisic acid, abscisic acid catabolites and analogs. J. Plant Growth Regul. 24, 274–284

Zhao, S., Fernald, R.D., 2005. Comprehensive algorithm for quantitative real-time polymerase chain reaction. J. Computl. Biol 12, 1047–1064.

Zhang, J., Davies, W.J., 1989. Abscisic acid produced in dehydrating roots may enable the plant to measure the water status of the soil. Plant Cell Environ. 12, 73–81.

Zhang, Y., Yang, J., Lu, S., Cai, J., Guo, Z., 2008. Overexpressing SgNCED1 in tobacco increases ABA level, antioxidant enzyme activities, and stress tolerance. J. Plant Growth Regul. 27, 151–158.

Zhang, F.P., Sussmilch, F., Nichols, D.S., Cardoso, A.A., Brodribb, T.J., McAdam, S.A.M., 2018. Leaves, not roots or floral tissue, are the main site of rapid, external pressure-induced ABA biosynthesis in angiosperms. J. Exp. Bot. 69, 1261–1267.

Zandalinas, S.I., Rivero, R.M., Martínez, V., Gómez-Cadenas, A., Arbona, V., 2016. Tolerance of citrus plants to the combination of high temperatures and drought is associated to the increase in transpiration modulated by a reduction in abscisic acid levels. BMC Plant Biol. 16, 105.

Tables

Table 1. List of gene primers used for qRT-PCR analysis in *Citrus limonia*.

Gene abbreviation	Gene name	Forward (5'-3')	Reverse (5'-3')	References
GAPC2	Glyceraldehyde-3-phosphate dehydrogenase	5′-TCCTATGTTTGTTGTGGGTG-3′	5′-GGTCATCAAACCCTCAACAA-3′	Mafra *et al.*, 2012; Silva *et al.*, 2019
EFα	Elongation factor 1-alpha	5′-TCAGGCAAGGAGCTTGAGAAG-3′	5′-GGCTTGGTGGGAATCATCTTAA-3′	Mafra *et al.*, 2012; Silva *et al.*, 2019
NCED1	9-cis-epoxycarotenoid dioxygenase 1	5′-GACCAGC AAGTGGTGTTCAA-3′	5′-AGAGGTGGAAACAGGAGCAA-3′	Bassene *et al*., 2009; Neves *et al*., 2013
NCED3	9-cis-epoxycarotenoid dioxygenase 3	5′-GGAGAATGAGGATGATGGCTAC-3′	5′-CTTTCGCGCTTATGAACGTG-3′	Agusti *et al*., 2007; Neves *et al*., 2013
NCED5	9-cis-epoxycarotenoid dioxygenase 5	5′-CTTCCCAACGAAGT CCATAG-3′	5′-GGATTCCATTGTGATTGCTG-3′	Agusti *et al*., 2007; Neves *et al*., 2013

Figure legends

Fig. 1. Main root length (A), root surface area (B), root diameter (C) and root biomass (D) of *C. limonia* grown for 90 days in nutrient solution containing 0 and 1480 μM Al. For each evaluation date, asterisks indicate significant differences ($P < 0.05$) between 0 and 1480 μM Al. For plants not exposed to Al, distinct uppercase letters indicate significant differences ($P < 0.05$) between 0 and 90 DAT; for plants exposed to Al, distinct lowercase letters indicate significant differences ($P < 0.05$) between 0 and 90 DAT. Columns are mean values (n = 6, ± SE).

Fig. 2. Leaf number (A), area (B) and biomass (C) of *C. limonia* grown for 90 days in nutrient solution containing 0 and 1480 μM Al. For each evaluation date, asterisks indicate significant differences ($P < 0.05$) between 0 and 1480 μM Al. For plants not exposed to Al, distinct uppercase letters indicate significant differences ($P < 0.05$) between 0 and 90 DAT; for plants exposed to Al, distinct lowercase letters indicate significant differences ($P < 0.05$) between 0 and 90 DAT. Columns are mean values (n = 6, ± SE).

Fig. 3. Leaf gas exchange and water use efficiency of *C. limonia* grown for 90 days in nutrient solution containing 0 and 1480 μM Al. (A) CO_2 assimilation, (B) stomatal conductance, (C) transpiration, (D) intercellular CO_2, (E) water use efficiency and (F) intrinsic water use efficiency. For each evaluation date, asterisks indicate significant differences ($P< 0.05$) between 0 and 1480 μM Al. Circle symbols are mean values (n = 6, ± SE).

Fig. 4. Leaf water potential at predawn (Ψ_{pd}) (A) and midday (Ψ_{md}) (B) of *C. limonia* grown for 90 days in nutrient solution containing 0 and 1480 μM Al. For each evaluation date, asterisks indicate significant differences ($P< 0.05$) between 0 and 1480 μM Al. Circle symbols are mean values (n = 4, ± SE).

Fig. 5. Relative leaf water content (A) and estimated hydraulic conductance from roots to the leaf (B) of *C. limonia* grown for 90 days in nutrient solution containing 0 and 1480 μM Al. For each evaluation date, asterisks indicate significant differences ($P< 0.05$) between 0 and 1480 μM Al. Circle symbols are mean values (n = 6, ± SE).

Fig. 6. Foldchange of normalized expression level of *ClNCED1*, *ClNCED3* and *ClNCED5* in leaves (A, C, E, respectively) and root tips (B, D, F, respectively) of *C. limonia* grown for 90 days in nutrient solution containing 0 and 1480 μM Al. For each evaluation date, asterisks indicate significant differences ($P < 0.05$) between 0 and 1480 μM Al.The dotted line represents the control group, showing always the mean value of 1, and foldchange is that between control and Al treatment.Circle symbols are mean values (n = 4, ± SE).

Fig. 7. Abscisic acid (ABA) and its metabolites in leaves (left columns) and roots (right columns) of *C. limonia* grown for 90 days in nutrient solution containing 0 and 1480 μM Al. For each evaluation date, asterisks indicate significant differences ($P < 0.05$) between 0 and 1480 μM Al. Circle symbols are mean values (n = 4, ± SE). (PA: phaseic acid; DPA: dihydrophaseic acid; 7′OHABA: (+)-7′-hydroxy-abscisic acid; ABA-GE: abscisic acid glucosyl ester).

Fig 8. Aluminum concentration in leaves (A) and roots (B) of *C. limonia* grown for 90 days in nutrient solution containing 0 and 1480 μM Al. For each evaluation date, asterisks indicate significant differences ($P < 0.05$) between 0 and 1480 μM Al. For plants not exposed to Al, distinct uppercase letters indicate significant differences ($P < 0.05$) between 0 and 90 DAT; for plants exposed to Al, distinct lowercase letters indicate significant differences ($P < 0.05$) between 0 and 90 DAT. Columns are mean values (n = 6, ± SE).

Appendix A. Supplementary data

Additional supporting information may be found in the online version of this article.

Fig. S1. Morphological details of shoots, leaves and roots of *C. limonia* grown for 90 days in nutrient solution containing 0 (on the left) and 1480 μM Al (on the right).

Fig. S2. Individual readings (replicates; n = 4 plants) of leaf abscisic acid concentration ($[ABA]_{leaf}$) and *ClNCED3* expression (Foldchange) in *C. limonia* grown for 90 days in nutrient solution containing 1480 μM Al.

Fig. S3. Individual readings (replicates; n = 4 plants) of leaf abscisic acid concentration ($[ABA]_{leaf}$) and stomatal conductance (*gs*) in *C. limonia* grown for 90 days in nutrient solution containing 0 and 1480 μM Al.

Highlights:

Aluminum (Al) toxicity inhibits root growth and reduces the stomatal conductance (*gs*)

The 9-*cis*-epoxycarotenoid dioxygenase (NCED) enzyme catalyzes the abscisic acid (ABA)

Roots of *Citrus limonia* exposed to Al up-regulated *ClNCED3* before *gs* was reduced

Up-regulation of *ClNCED3*, *ClNCED1* and *ClNCED5* matched ABA leaf levels

Al triggers ABA biosynthesis, which is associated with the low *gs*

Figure

Click here to access/download;Figure;Figure 1 - citrus_root groth.tif

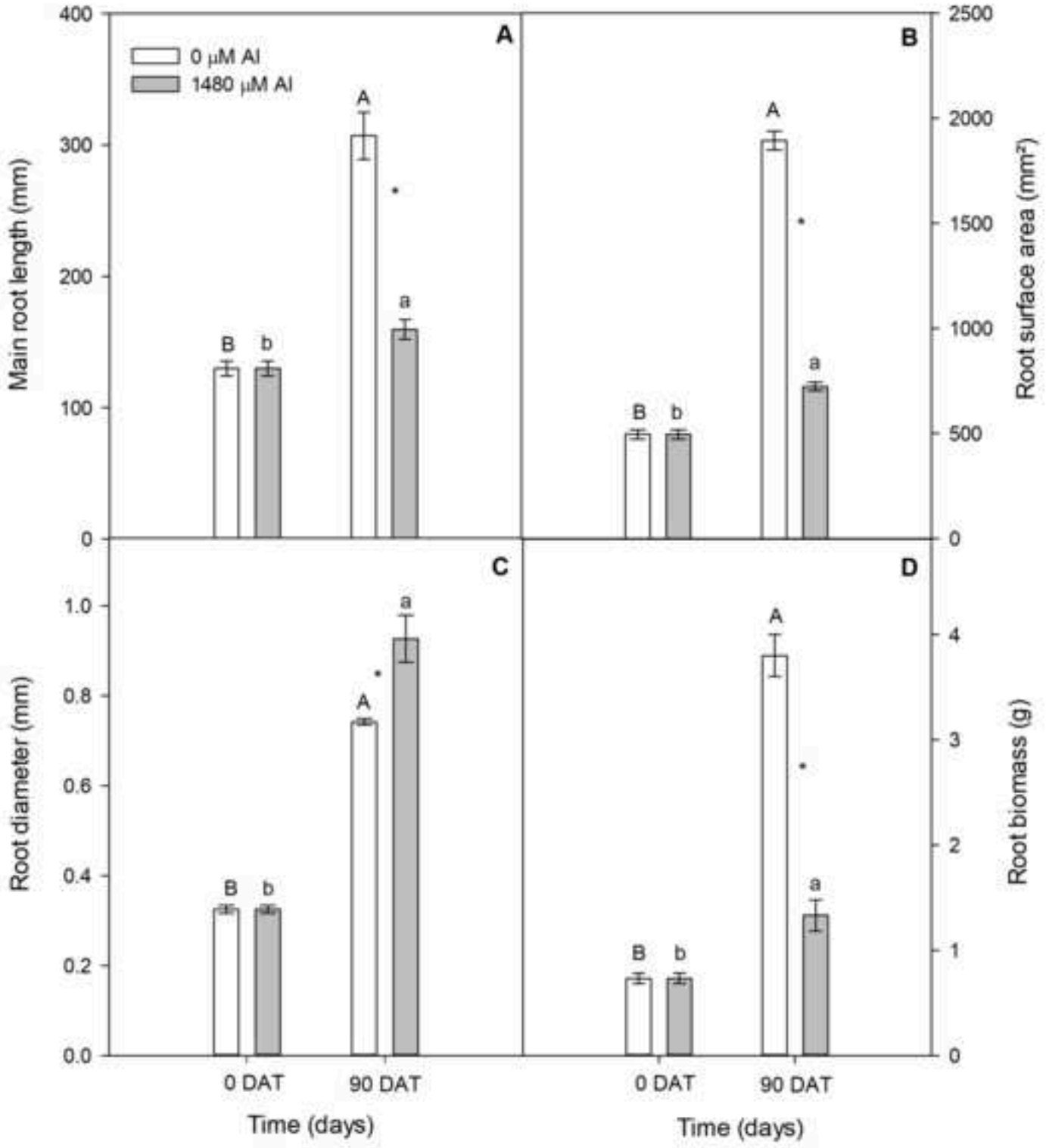

Figure

Click here to access/download;Figure;Figure 2 - citrus_leaf growth.tif

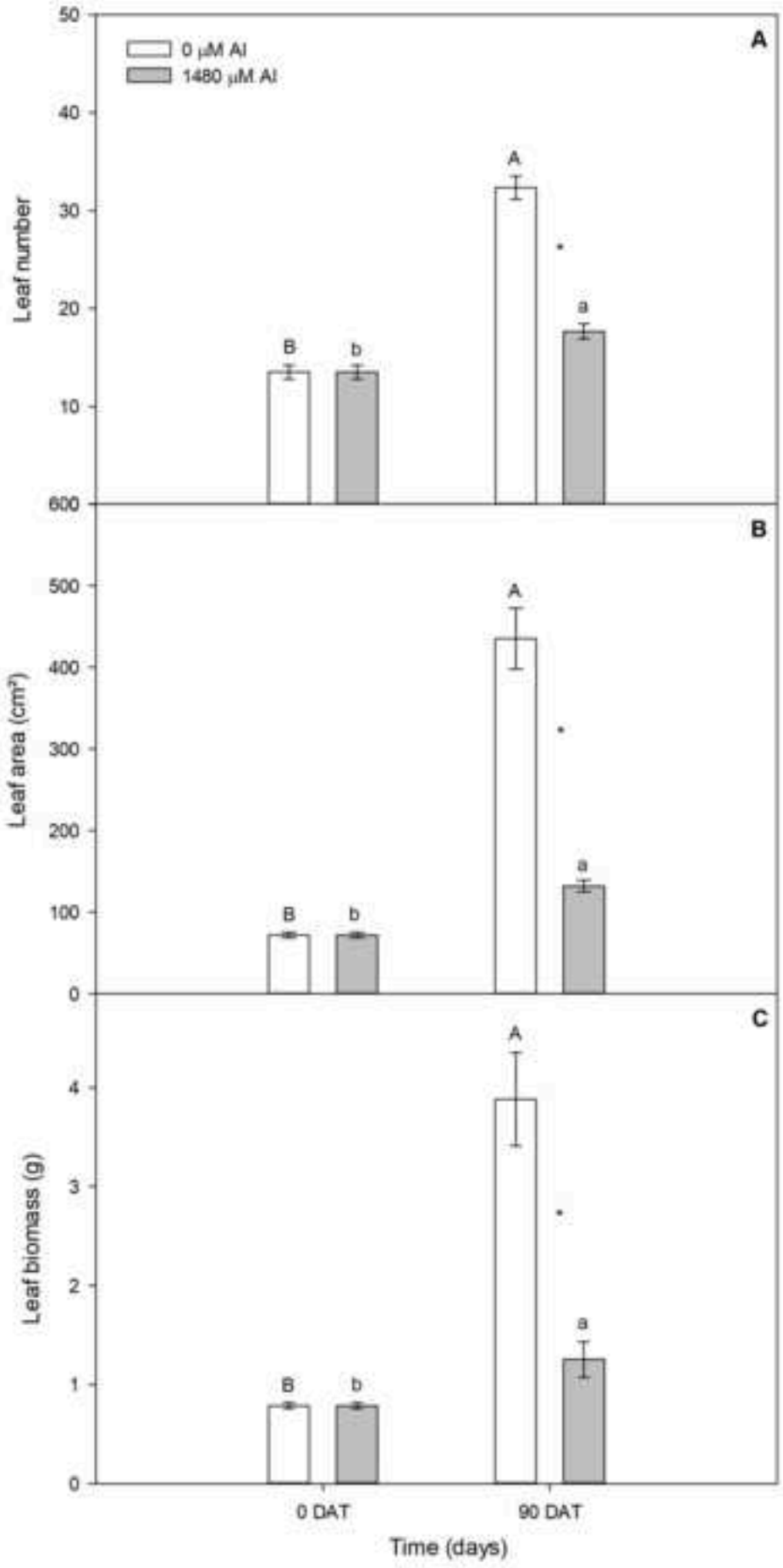

Figure

Click here to access/download;Figure;Figure 3_citrus_gas exchange.tif

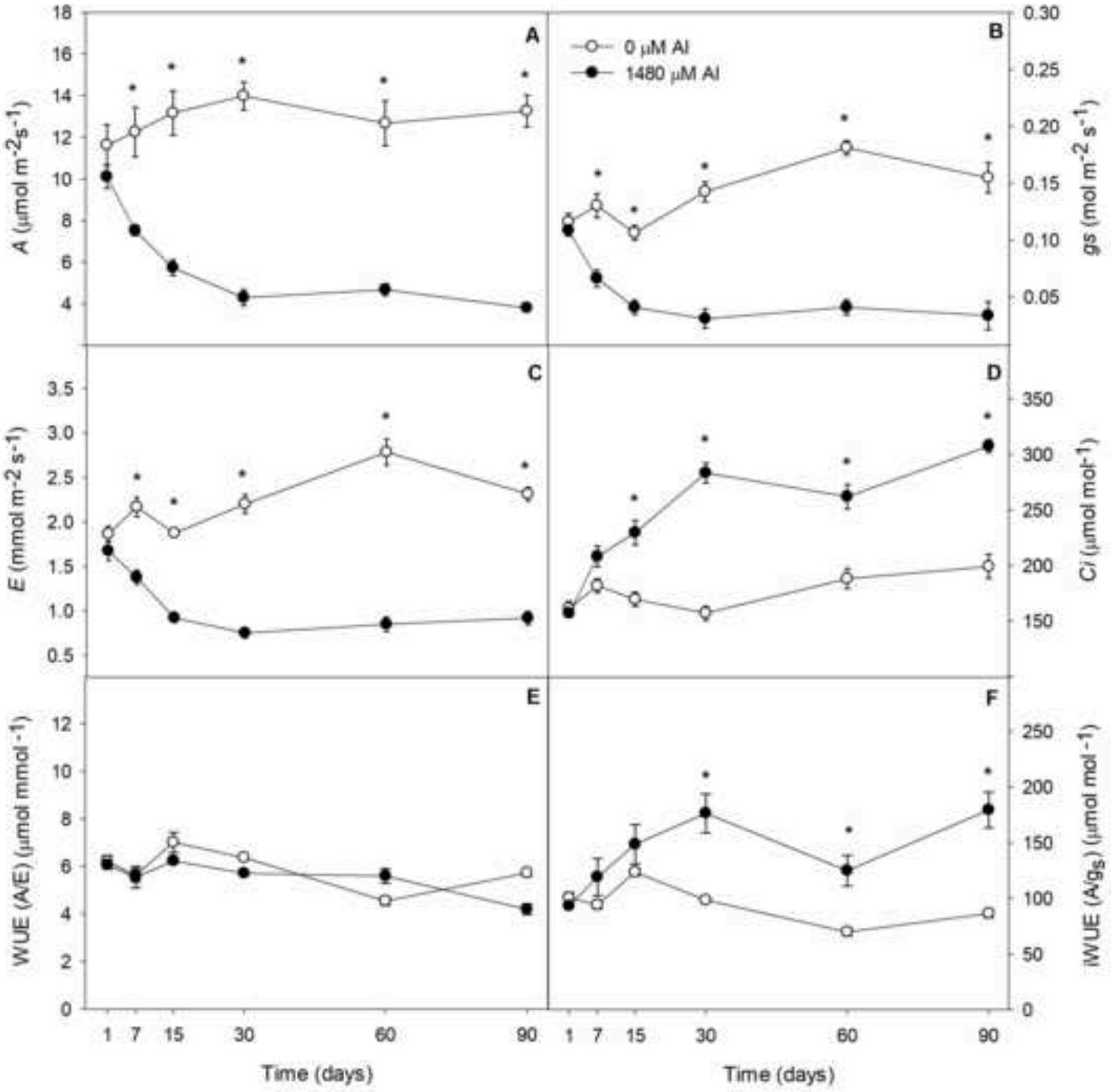

Figure

Click here to access/download;Figure;Figure 4 - citrus_water potential.tif

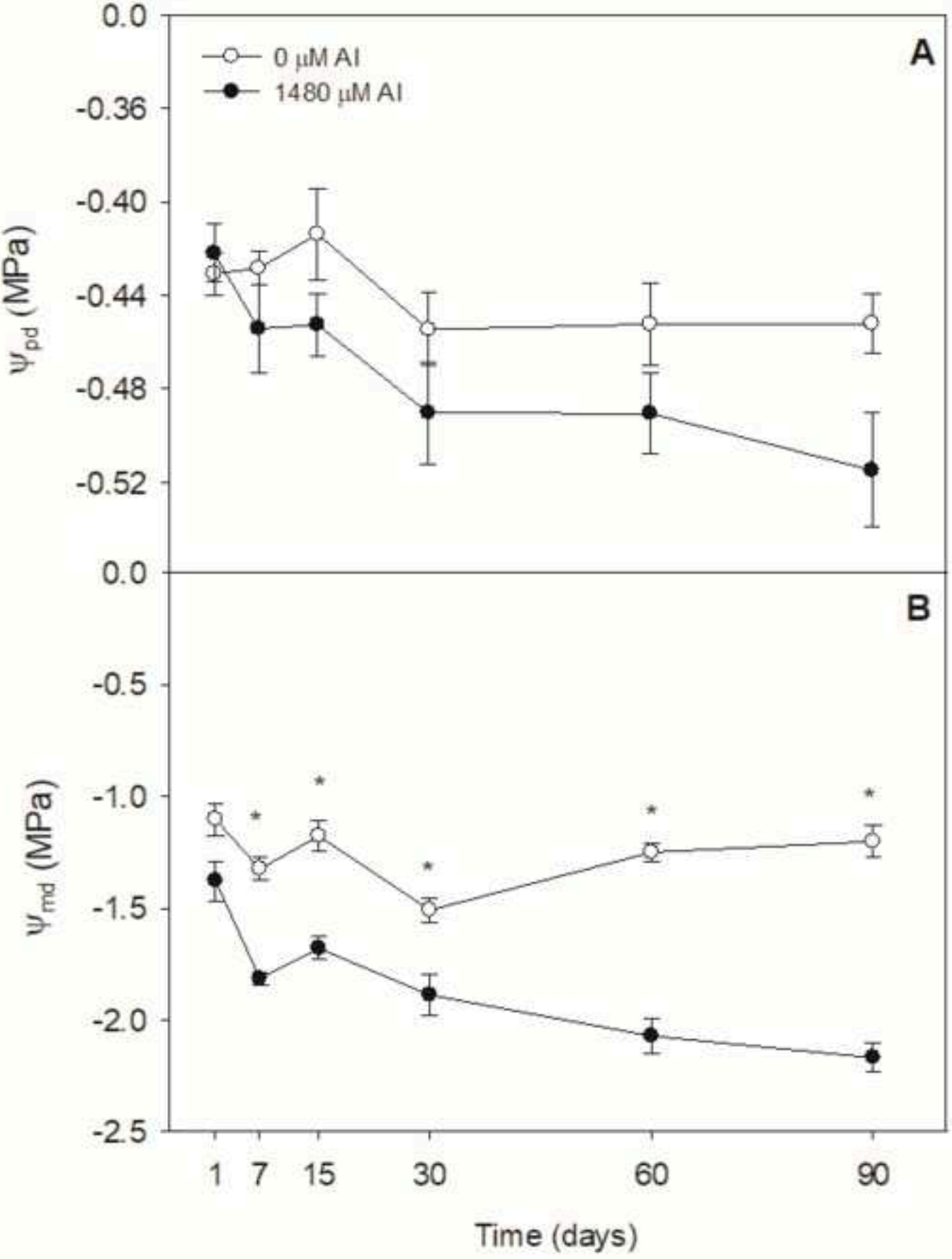

Figure

Click here to access/download;Figure;Figure 5 - RWC and KL.TIF

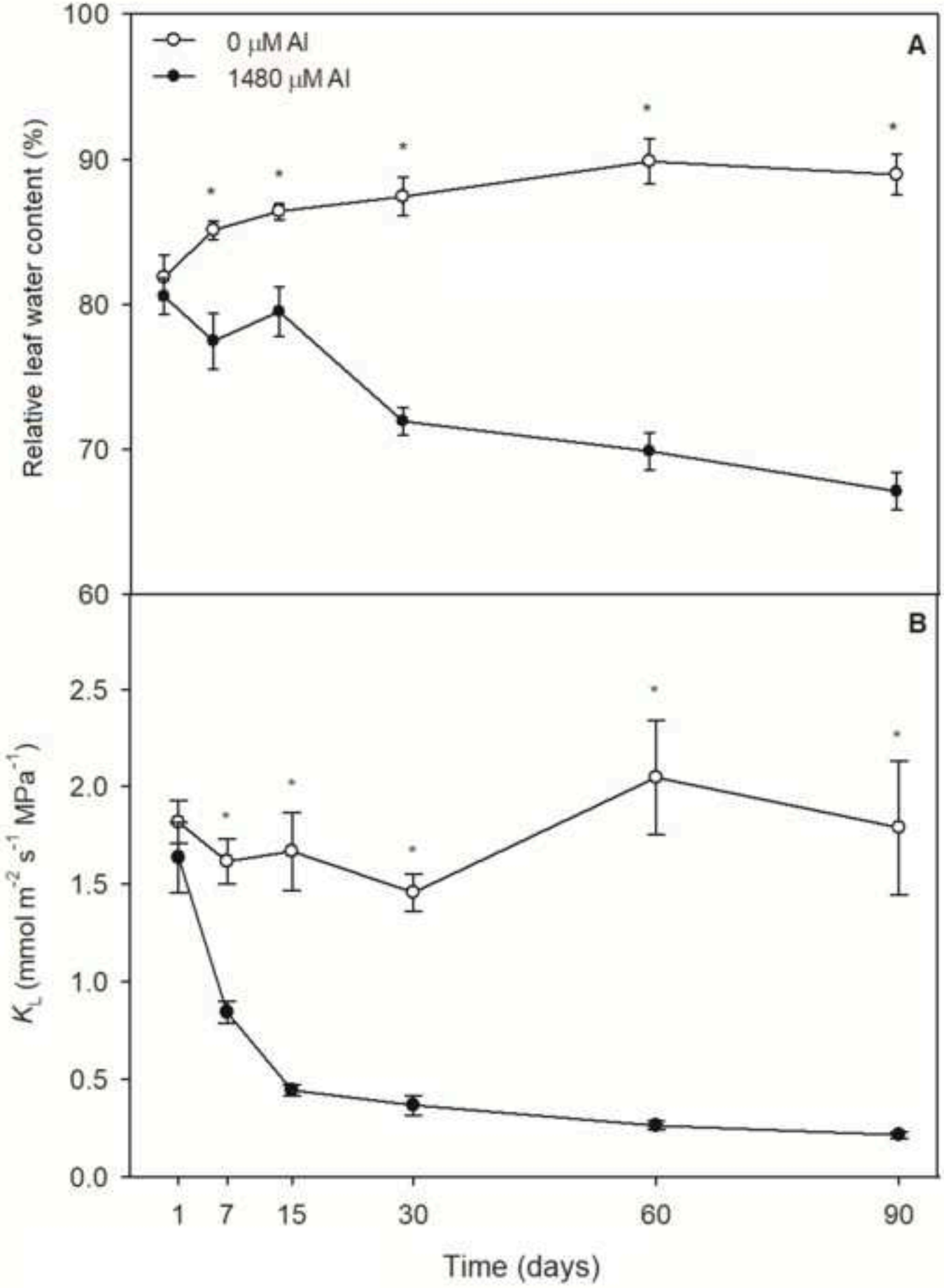

Figure

Click here to access/download;Figure;Figure 6 - NCED todas.tif

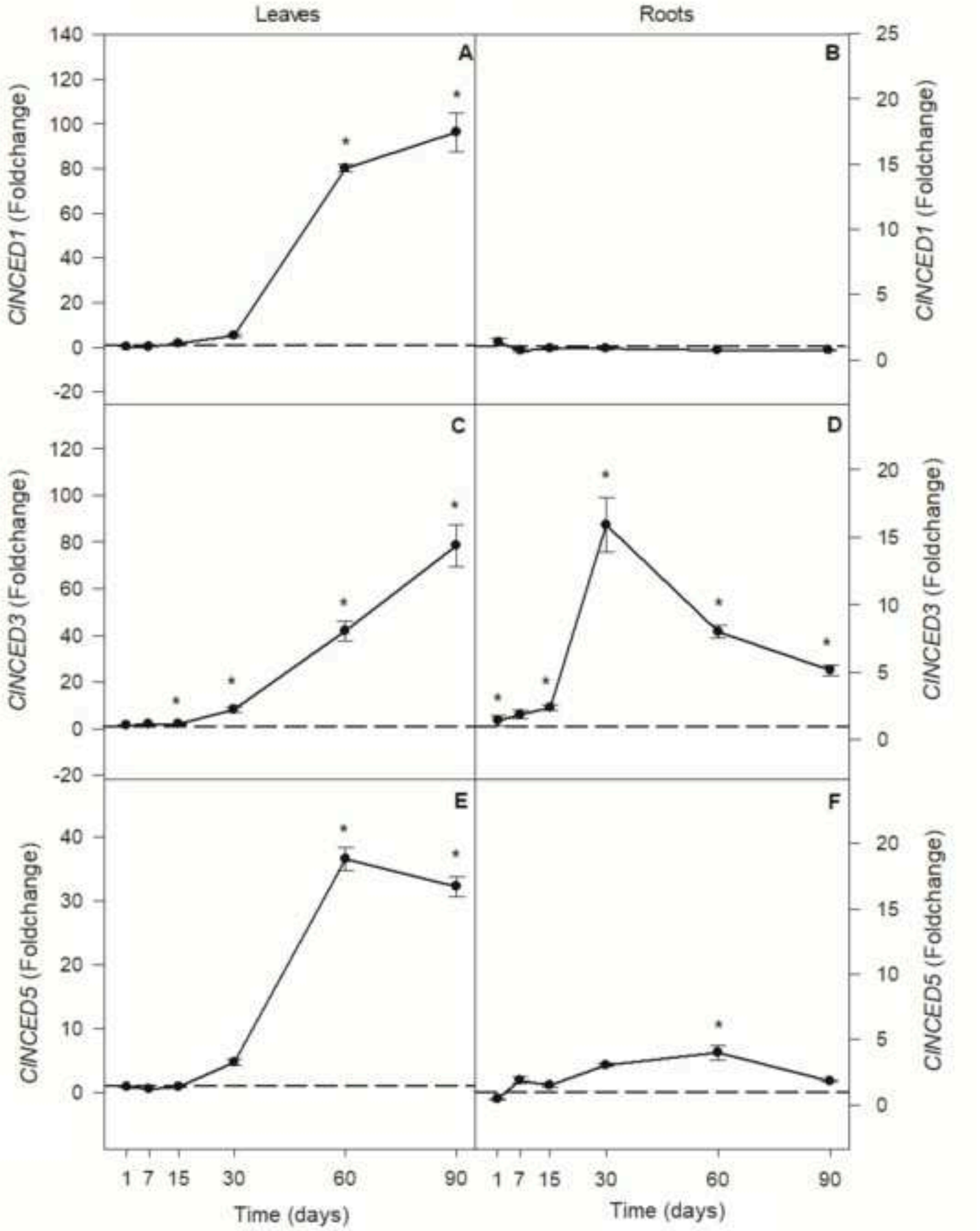

Figure

Click here to access/download;Figure;Figure 7 - ABA METABOLITES.tif

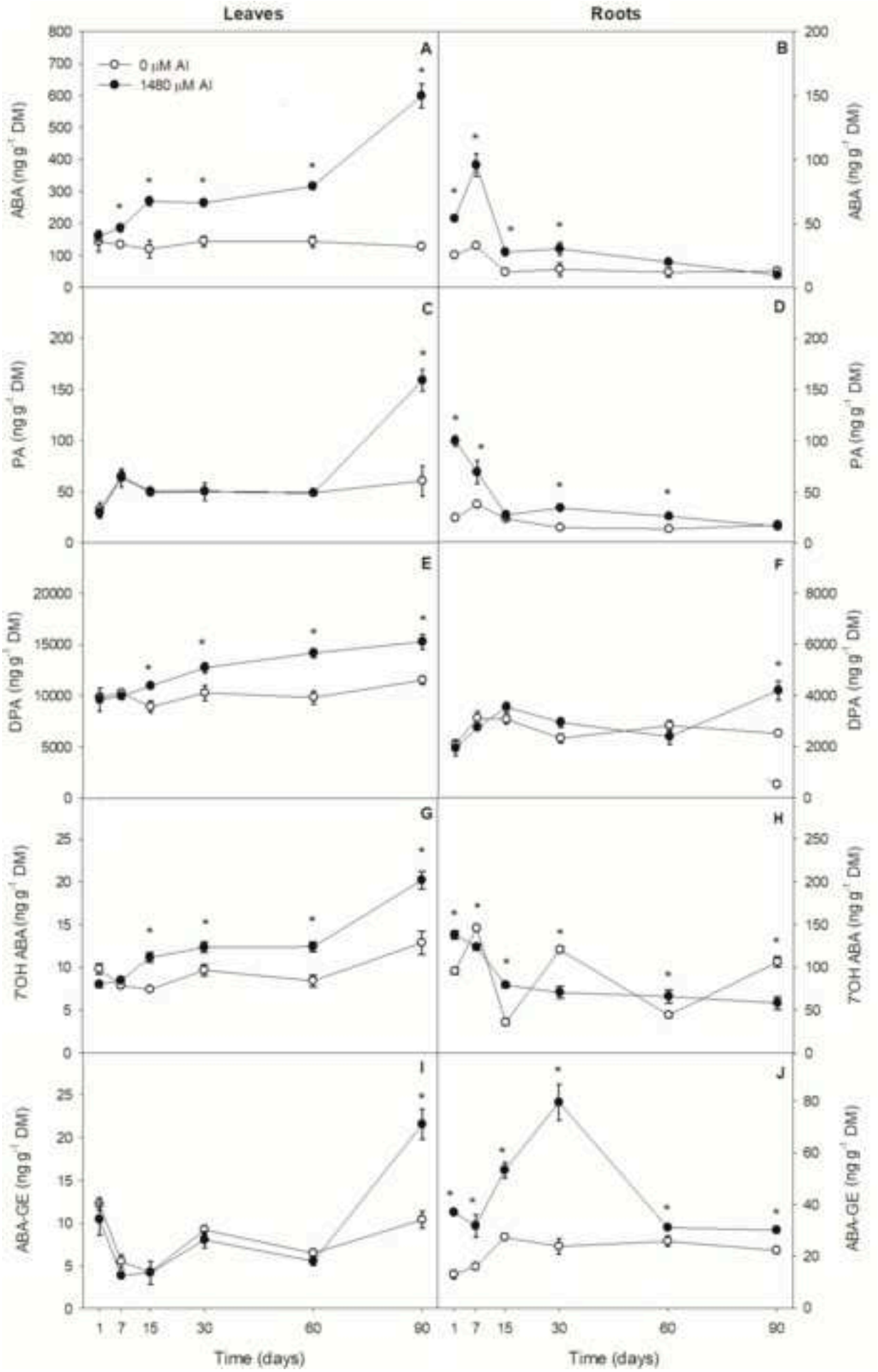

Figure

Click here to access/download;Figure;Figure 8 - Al concentration corrected.tif

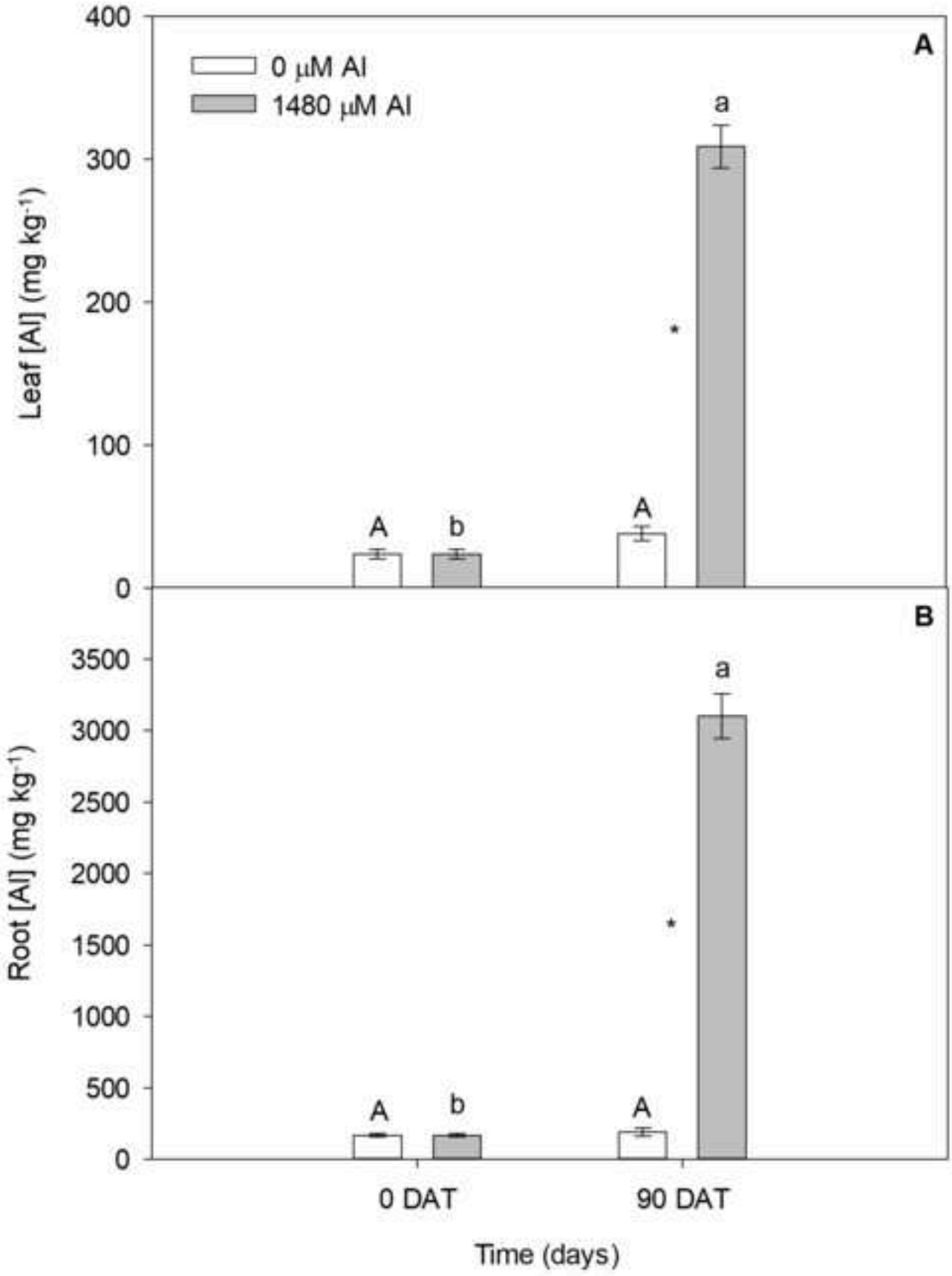

Figure

Click here to access/download;Figure;Supplementary Figure S1 - plants_final.jpg

Figure

Click here to access/download;Figure;Supplementary Figure S2 - ABA leaf x NCED3 with regression.TIF

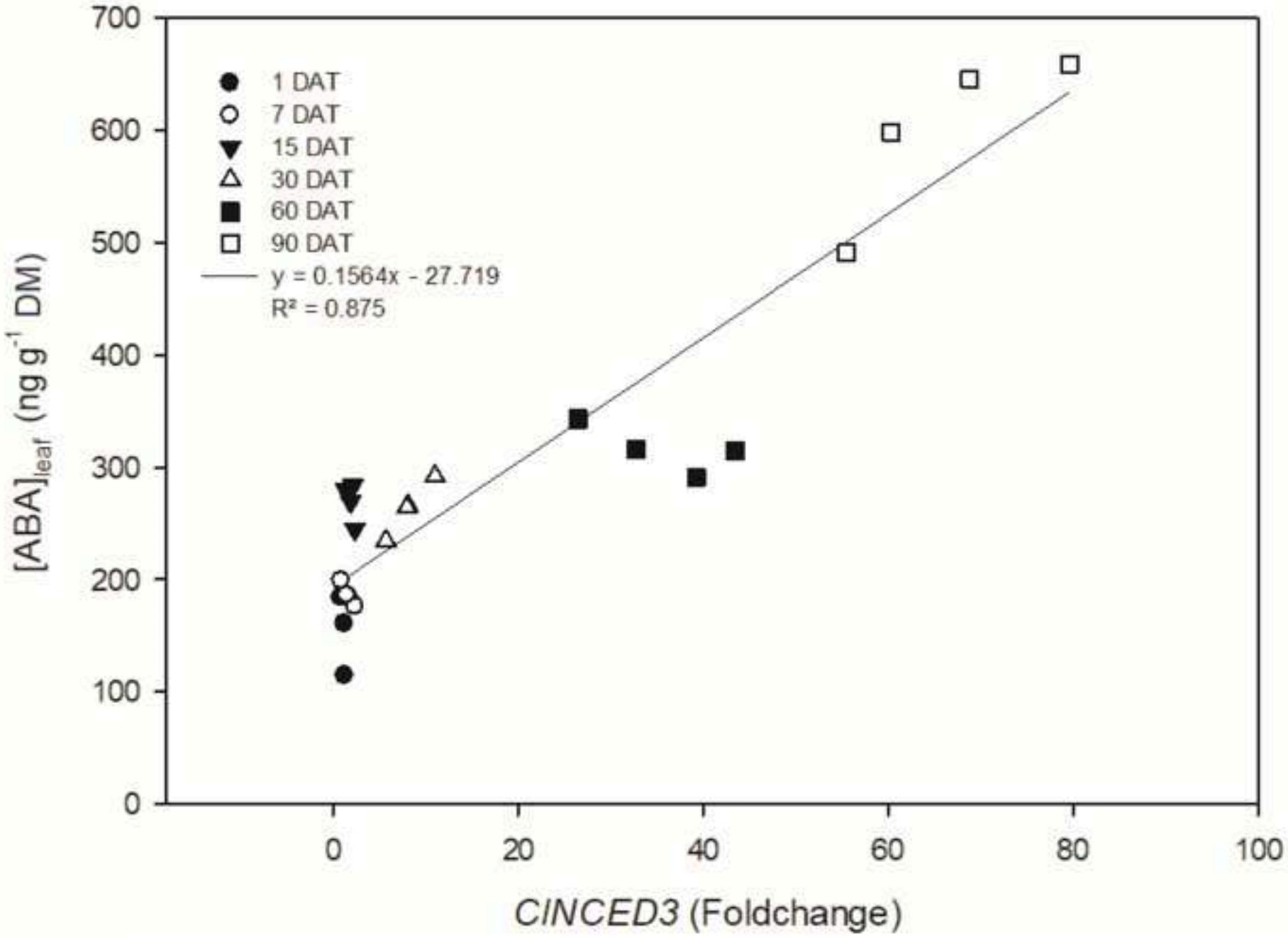

Figure

Click here to access/download;Figure;Supplementary Figure S3 - gs x ABAleaf.TIF